

Seasonal and inter-annual sea surface height variations of the northern Indian Ocean from the TOPEX/POSEIDON altimeter

S Prasanna Kumar

National Institute of Oceanography, Dona Paula, Goa 403 004, India

and

H Snaith, P Challenor & H T Guymer

James Rennell Division for Ocean Circulation, Southampton Oceanography Centre, Southampton, United Kingdom

Received 23 May 1997, revised 3 November 1997

The seasonal and inter-annual variability of the northern Indian Ocean was studied by analysing 10-day snapshots of sea surface height (SSH) data from TOPEX/POSEIDON altimeter for the period November 1992 to August 1995. The large scale SSH variations reflect the dominant seasonal signal such as the coastal currents, the upwelling zones along Somalia, Arabia and west coast of India, the Great Whirl and Southern Gyre, and eddies in the Bay of Bengal. Temporal evolution of the coastal circulation along the east and west coast of India, and offshore movement of the high (low) SSH patch during winter (summer) away from the tip of India indicates the role of remote forcings along the boundary and into the interior oceans. Inter-annual variability showed that during 1994 the winter time coastal current along the west coast of India was fully developed and intense, and upwelling signatures along Somalia and Arabia were the strongest.

The limited northern extent, the semi-annual monsoonal (summer to winter) wind reversal (south-west during June-September and north-east during November-February), the inflow of warm, high saline waters of the Persian Gulf and the Red Sea into the western region (Arabian Sea) and the large quantities of fresh water influx from the Peninsular India and low salinity Pacific Ocean Through Flow into the eastern region (Bay of Bengal); all these make the northern Indian Ocean a dynamically interesting region for study. Subsequent to the International Indian Ocean Expedition (IIOE, 1962-65), there had been numerous studies aimed at understanding the general hydrographic characteristics and circulation of the Indian Ocean. Though there exists a broad understanding of the general circulation, various aspects of circulation such as seasonal dependence and inter-annual variability are still not well understood. This is largely due to the paucity of data both spatially and temporally.

The major reference for Indian Ocean research, except in the Somali and Madagascar regions, still

remains the atlas of Wyrki¹ based on the IIOE data and that of Cutler & Swallow² using the ship drift. Some of the recent studies suggest the existence of semi-annual periodicities due to semi-annual reversal of wind³⁻⁵. The annual and semi-annual harmonics of the mixed layer depth and of the surface currents north of 30°S were described from the temperature profiles⁶ and drifters⁷. A major constraint in the study of low-frequency variability is the availability of long time-series data having sufficient spatio-temporal resolution. In view of this, the TOPEX/POSEIDON altimeter data was utilised for the present study to infer the seasonal and inter-annual variability of the northern Indian Ocean.

Materials and Methods

TOPEX/POSEIDON Altimeter

The TOPEX/POSEIDON (hereafter referred as T/P) satellite has two altimeters on board: the NASA (USA) dual-frequency radar altimeter (ALT) measuring at frequencies 5.3 and 13.6 GHz

and the CNES (France) single-frequency solid state radar altimeter operating at 13.65 GHz (for more details see AVISO User Handbook⁸). Launched on 10 August 1992, the science data acquisition started from 23 September 1992 (start of cycle 1). The satellite is at an altitude of 1336 km and the ground track (Fig.1) repeat period is 9.9 days with 316 km cross-track separation at the equator.

An altimeter operates by sending out a short radar pulse and measuring the time required for the pulse echo to return from the sea surface. This measurement, the altimeter range (Fig.2 A), gives a first estimate of the height of the instrument above the sea surface. To be oceanographically useful, the altimeter range need to be corrected so as to make it accurate within cm's. The sea surface height (SSH) is obtained by differencing the satellite's range to the sea surface and the computed height of the satellite's orbit above a reference ellipsoid (Fig.2 A).

Data processing

The T/P Indian Ocean data used in this study were extracted from the merged geophysical data records (MGDR), from AVISO CD-ROM, between longitudes 40°E to 100°E and latitudes 10°S to 30°N. In all 101 repeat cycles, from cycle 6 to 106, covering the period 11 November 1992 to 10 August 1995 were used in the analysis. The first 5 cycles were excluded from the analysis as there

were mispointing problems. The altimeter data extracted from the MGDRs consist of geolocated, 1-second average height estimates. There are various source of error in the altimeter height measurement. The MGDRs include a variety of corrections and data quality flags, which are discussed in detail by Callahan⁹.

The corrections applied to the T/P data for the present study are summarised in Table 1. The raw ionosphere corrections were averaged over a 21-s moving window as recommended by Callahan⁹ to eliminate high-frequency noise. In addition to these corrections, a bias of 14.5 cm was applied to TOPEX data to account for absolute measured bias. No orbit corrections were applied as the accuracy of the T/P orbits is at the same level as most of the measurement corrections¹⁰. Further, the data where the standard deviation of SSH, the significant wave height (SWH), and the automatic

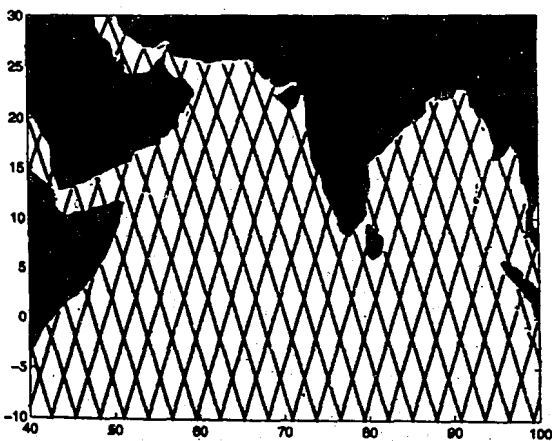


Fig. 1—Map showing the ground track of TOPEX/POSEIDON.

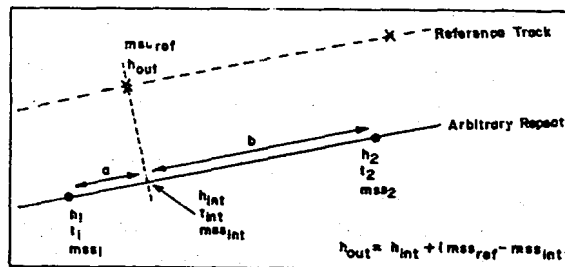
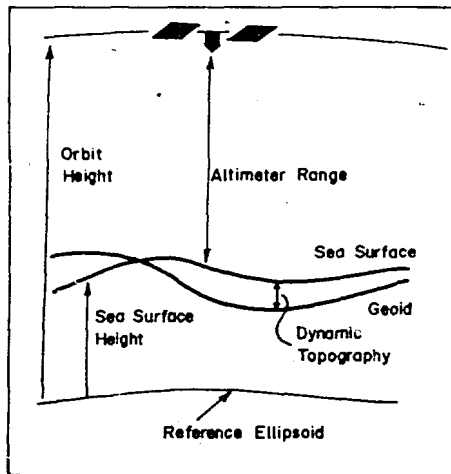


Fig.2—Schematic diagram showing A) the measurement of sea surface height using altimetry and B) the gradient reduction method (adopted from Jones¹⁹)

Table 1—Corrections applied to the TOPEX/POSEIDON altimeter data		
Corrections	TOPEX	POSEIDON
Dry tropospheric	ECMWF Model pressure field	
Wet tropospheric	TOPEX microwave radiometer	
Ionospheric	Dual frequency altimeter	DORIS
EMBias	Gasper model	
Inverse barometer	ECMWF Model pressure field	
Solid earth tide	Cartwright & Edden Model	
Ocean tide	Texas model CSR 3.0	
Polar tide	Wahr model	
Geoid height	OSU 91A Model	

gain control (AGC) exceed the following thresholds (representing the global statistics of the data) were eliminated.

$\sigma(\text{SSH}) > 10 \text{ cm}$

$\sigma(\text{SWH}) > 2 \text{ m}$

$\sigma(\text{AGC}) > 0.25 \text{ dbar}$

From the corrected SSH data, the model geoid height (the height of the ocean geoid relative to the reference ellipsoid) was removed. The SSH thus obtained, should in principle, contain only the dynamically important sea surface topography. But in practice inadequate knowledge of the geoid will retain some ambiguity. Finally this is also eliminated using a collinear analysis that provide only the temporal variations of the sea surface height.

Collinear differences

Due to the along track variation of the position of sampling of SSH, as it is organised in time, the corrected, geoid removed SSH are to be collocated with a reference grid. Cycle 18 was chosen as the reference for computing collinear differences because it is close to the nominal ground track.

Apart from along track variations in sampling positions, there are also cross-track variations as the satellite does not exactly repeat its ground track, which is usually kept within 2 km of the nominal path. This may introduce errors in the SSH if the cross-track geoid gradients are significant. In order to minimise this, a gradient

reduction correction¹¹ was used where the difference between a model mean sea surface at the reference point and the interpolated along track point (Fig.2, B) were added to the interpolated along track height values. The Rapp OSU91A mean sea surface model¹² was used for this purpose. It was found that the gradient reduction correction reduces the SSH, particularly in the region where the Ninety-Degree East Ridge is located, by 1 to 1.5 cm.

From the gradient reduced collocated SSH data, the mean was subtracted from individual SSH to obtain SSH anomaly. Finally these SSH anomalies were grided on to a regular one-degree longitude by one-degree latitude grid, using a Gaussian interpolation with 200 km as full-width-half-maxima and 400 km as search radius.

Results and Discussion

Seasonal variability-Winter monsoon

During November the SSH in the eastern Indian Ocean including the Bay of Bengal is 30 cm higher compared to the rest of the region (Fig.3a) indicating the setting in of the north-east monsoon flow in response to the north-easterly trade winds. Along the eastern periphery the surface flow is towards north, as could be seen from the high SSH anomaly which continues along the east coast of India, where the current is southerly. In the Bay of Bengal, the low SSH near the western region indicates a geostrophically balanced large cyclonic circulation. Along the west coast of India, the surface current begins to flow towards the north from the southern tip. The relatively high SSH near the coast of Arabia and Somalia manifests the beginning of southerly surface currents along the western boundary. South of peninsular India, the north equatorial current (NEC), specially in the eastern region, starts flowing towards west. The signature of the south equatorial current (SEC) is identified as a band of high SSH along 10°S, specially in the eastern and western region.

In December, the high SSH seen in the eastern region starts weakening, but along the west coast of India the height increases and extends right up to the north (Fig.3b). Accordingly the surface current strengthens and move northward hugging

the coast into the prevailing weak north-easterlies. The low SSH in the northern Arabian Sea is due to the cold, denser waters associated with the winter cooling active during this period¹³. By the end of December and beginning of January the currents along the east coast of India north of 18°N begin to reverse and flow towards north (Fig.3c) as the band of high SSH disappear from the eastern Indian Ocean. Two anticyclonic eddies develop by the end of January near the north-western and south-western Bay (Fig.3d). Along the west coast of India, the SSH is highest during January, indicating that the northward coastal current attains its highest speed, heading into the weak local longshore wind during this time of the year. The current is now broader than in November, specially in the south, suggesting that it is no longer coastally trapped. The westward surface flow associated with the north-east monsoon is well established every where north of the Equator.

In the eastern Indian Ocean and most of the Bay of Bengal, the SSH becomes low in February (Fig.3e). Along the east coast of India, the low SSH present in the south-western corner, during the previous months disappears. The appearance of high sea level in place of low could be linked to local forcing by Ekman pumping. This drives a narrow northward coastal current along the east coast of India at this time of the year. Based on the AVHRR data Legeckis¹⁴ reported the presence of a western boundary current and later Shetye *et al.*¹⁵, using hydrographic data, proposed that the western boundary current forms a part of the seasonal anticyclonic sub-tropical gyre which fully develops during March-April. In the present case we noticed the prevalence of fully developed anticyclonic gyre till May.

When the north-east monsoon weakens in March, the western Bay and the entire Arabian Sea is almost covered by high SSH (Fig.3f). Anticyclonic circulation develops in the Bay and becomes fully established by April (Fig.3g). But along the west coast of India, the northerly coastal current begins to weaken by March. In fact, with the weakening of north-easterly winds, most of the circulation is the remnants of the earlier flow. Along the western boundary, the southerly flow continues with strength, especially along the

Somali coast which is maintained by the advection of the high SSH from Indian coast as well as the north-easterly winds still persisting along this region during March. In the equatorial region, by the end of February and beginning of March, when the equatorial winds are strong and organised westerlies, the high SSH seen along the western margin starts spreading towards the east. This is associated with the propagation of equatorial Kelvin waves. Similar propagational feature were identified by Prasanna Kumar & Unnikrishnan⁵ and Unnikrishnan *et al.*¹⁶, based on temperature climatology.

Summer monsoon

South-west monsoon winds sets in the Arabian Sea by May and the sea level also responds to the changed wind conditions. Along the Somali coast, the southward flowing winter time Somali current reverses to a northward flow (Fig.3h). Along the coast of Arabia, the flow is weak but northward. A region of shallow SSH appears along the west coast of India indicating a southerly coastal current. The upper layer thickness of the interior Arabian Sea increases. In the Bay of Bengal, along the east coast of India, in response to the strong upwelling-favourable south-westerly winds, the SSH thickness decreases north of 10°N and strengthens the northward current seen developing during March-April as a part of the anticyclonic circulation. The observed high SSH in the eastern equatorial Indian Ocean is linked to the propagation of equatorial Kelvin wave^{5,16}.

The high SSH seen in the eastern Indian Ocean spreads along the eastern boundary into the Bay of Bengal in June (Fig.3i). At this time, the large anticyclonic circulation splits into two gyres. In the Arabian Sea, along the Somali coast the development of Southern Gyre centred around 3°N and the formation of Great Whirl centered around 9°N takes place in the first week of June. By end of June the Southern Gyre appears to coalesce with the Great Whirl (Fig.3i). The upper layer thickness of the interior Arabian Sea increases further as a result of large scale downwelling associated with positive windstress curl.

In July when the southwest monsoon reaches its peak, the Somali current is in its full strength with

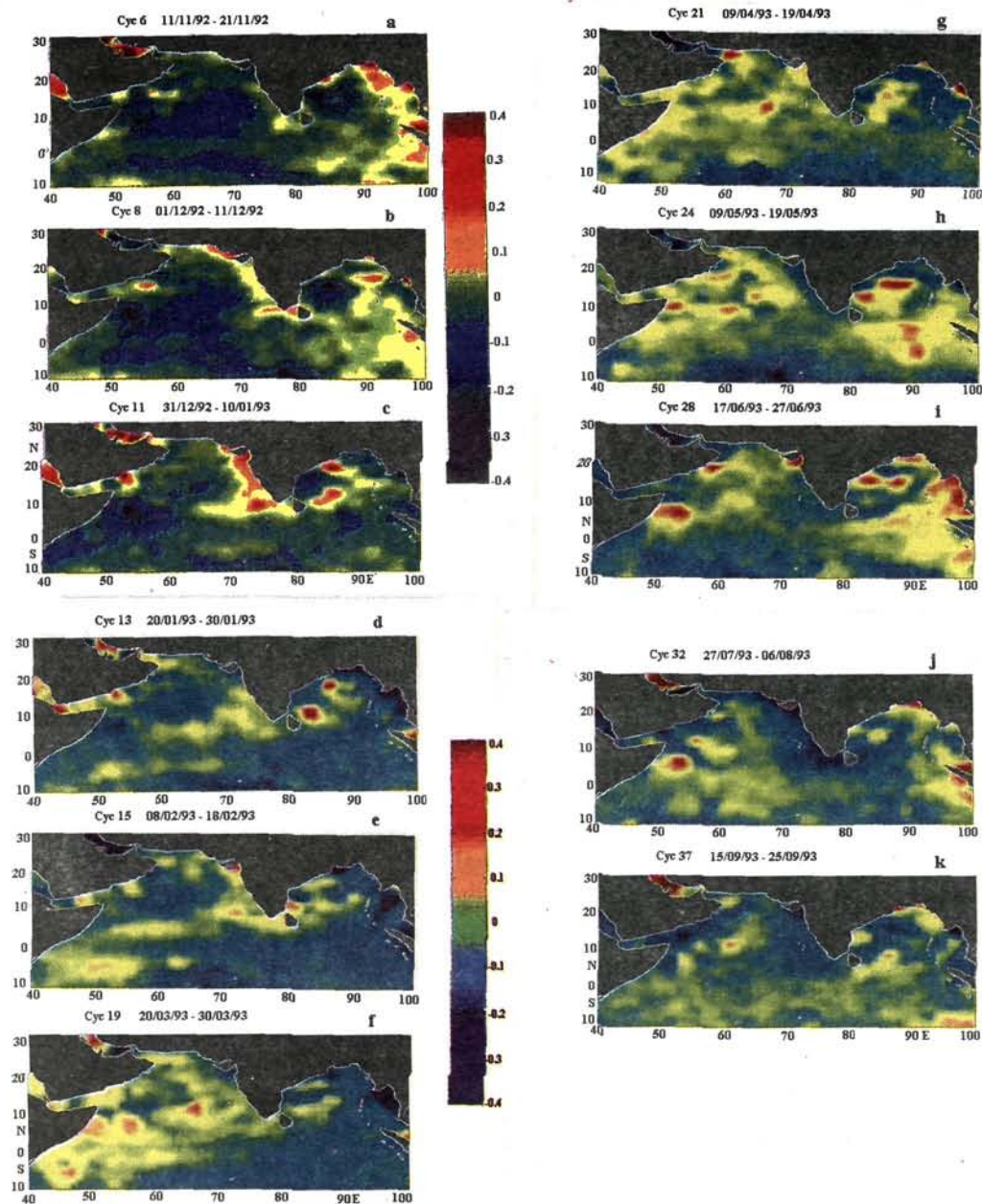


Fig.3—Ten-day snap shot of SSH anomaly maps derived from TOPEX/POSEIDON for cycles 6 (a), 8 (b), 11 (c), 13 (d), 15 (e), 19 (f), 21 (g), 24 (h), 28 (i), 32 (j) and 37 (k). (Colour bar is in meters)

upwelling established along Somalia, Arabia and south-west coast of India as indicated by the low SSH (Fig.3j). North-east of Great Whirl another eddy is seen, which appears to be the Socotra eddy displaced east by the advection of Somali current away from the coast. Along the west coast of India the upwelling front propagates offshore much faster in the south than north indicating that it is no longer coastally trapped. Based on hydrography and current measurements, Antony & Unnikrishnan¹⁷ reported the offshore movement of the upwelling front from July to September. In the Bay of Bengal, spreading of high SSH along the eastern boundary seen during June, reaches up to 18°N and below it, along the east coast of India, low SSH indicates a southward pressure gradient force in the upper layers. The picture remains more or less similar in August.

With the weakening of the south-west monsoon winds in September, the Somali current weakens and Socotra Eddy disappears (Fig.3k). In the Bay of Bengal low SSH prevails in most of the region. With the collapse of south-westerly winds in

October along the equator, once again the organised westerlies prevail. In the Arabian Sea, the SSH distribution is similar to that in September except with the reappearance of a warm core eddy east of Socotra region and a couple of weaker and smaller ones north-east of it. In the Bay of Bengal, cyclonic circulation starts developing in the eastern side of it.

Inter-annual variability

In order to decipher the inter-annual variability, monthly mean SSH anomaly maps of January and July representing the winter and summer monsoon respectively were constructed for the year 1993, 94 and 95. During 1993 January (Fig.4A, upper panel), the surface circulation in the Bay of Bengal is anticyclonic close to the south-western region. The northward coastal current along the west coast of India is fully developed. The offshore propagation of SSH from the southern tip of India reaches up to 60°E. Winter cooling is seen as a region of low SSH in the northern Arabian Sea. The SEC is not seen as a strong signal. On the contrary, during 94

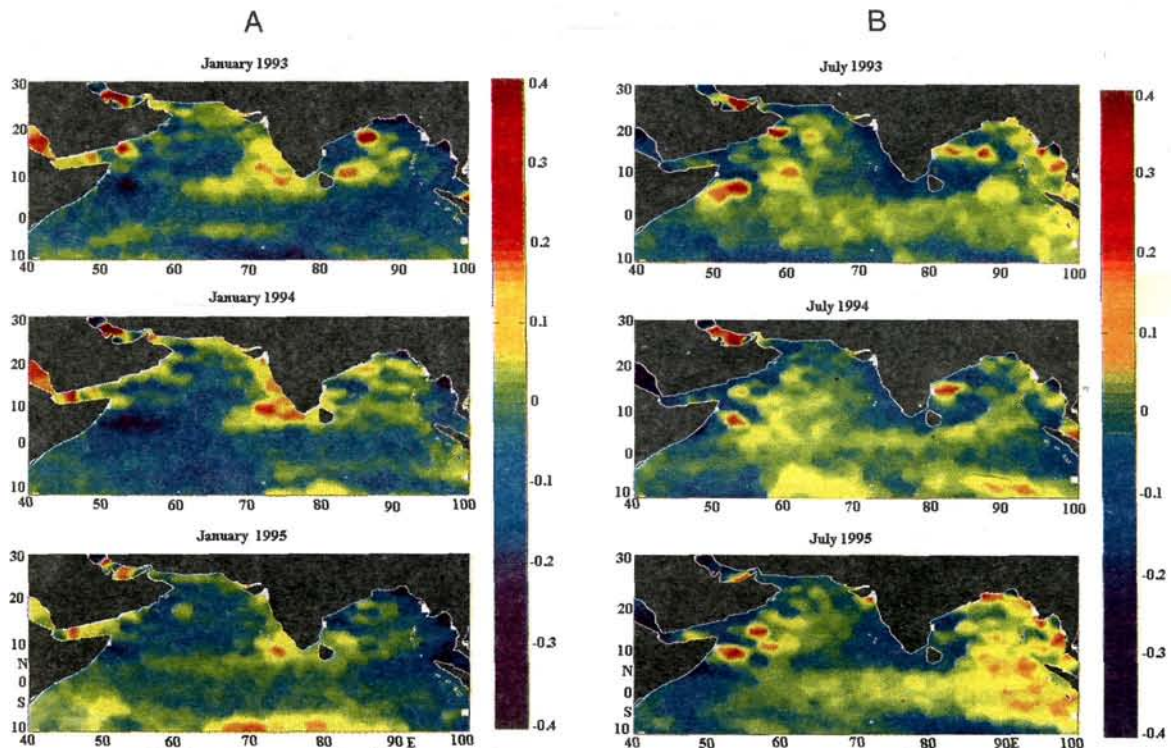


Fig.4—Monthly mean SSH anomaly maps for A) January and B) July

the surface circulation in the most parts of the Bay is cyclonic, the northward coastal current along the west coast is much stronger and coherent (Fig.4A, middle panel). However, the offshore extension of the high SSH is seen limited to 65°E. The signature of SEC is prominently seen along 10°S between 70°E and 85°E. In 95 the anticyclonic circulation is weak in the Bay of Bengal and the coastal current along the west coast of India is in the formative stage (Fig.4A, lower panel). However, the SEC appears as a distinctive band of high SSH along 10°S.

During 1993 July, along the Somali coast, Southern Gyre as well as the Great Whirl is seen in a coalescing stage apart from another eddy along the northern Arabia (Fig.4B, top panel). A patch of low thickness extends from the tip of India into the interior Arabian Sea up to 63°E. In the Bay of Bengal the spreading of high SSH along the eastern boundary is seen up to 18°N with a thick band of high SSH in the equatorial belt from 50°E right up to the eastern region. Contrastingly, in 94 July, strong upwelling is seen along Somalia and Arabia ; the Great Whirl is much weaker and smaller in spatial extent. The spatial extent of the low SSH patch from the tip of India is only up to 70°E (Fig.4B, middle panel). The band of thick SSH seen in the equatorial belt is shifted to north and is weak, but it does not occupy the eastern region. Accordingly, the spreading of SSH along the eastern boundary is also not well defined. A mesoscale anticyclonic circulation feature is identified near the south-western Bay. Signatures of SEC is noticed east of 60°E along 10°S which is not discernible either in 1993 or 1995 July. In 95 July, the Great Whirl is once again active and another anticyclonic eddy is seen north of this (Fig.4B, bottom panel). The low SSH patch from the tip of India extends up to 60°E. The entire Bay of Bengal and the eastern region east of 83°E is covered by thick SSH. The observed inter-annual variability showed marked resemblance with the propagational characteristics of the Kelvin and Rossby waves in the Indian Ocean¹⁸.

Acknowledgement

SPK is grateful to the Director, NIO for his support, to David Cromwell & Matthew Jones for providing the software and to the Indian National

Science Academy (INSA) and Royal Society for providing the fellowship. This paper is NIO contribution number 2546.

References

- 1 Wyrski K, *Oceanographic atlas of the International Indian Ocean Expedition*, (National Science Foundation, Washington DC) 1971, pp. 531.
- 2 Cutler A N & Swallow J C, *Surface currents of Indian Ocean*, Report no.187, (Institute of Oceanographic Sciences, Bracknell, UK), 1984, pp. 8.
- 3 Gent P K, O'Neill K & Cane M A, *J Phys Oceanogr*, 13 (1983) 2148.
- 4 Clarke A J & Liu X, *J Phys Oceanogr*, 23 (1993) 386.
- 5 Prasanna Kumar S & Unnikrishnan A S, *J Geophys Res*, 100 (1995) 13585.
- 6 Rao R R, Molinari R L & Festa J F, *J Geophys Res*, 94 (1989) 10801.
- 7 Molinari R L, Olson D & Reverdin G, *J Geophys Res*, 95 (1990) 7217.
- 8 AVISO User Handbook: Merged TOPEX/POSEIDON products, Report AVI-NT-02-101-CN, 2nd ed., (CNES, Toulouse, France) 1992, pp. 208.
- 9 Callahan P S, TOPEX/POSEIDON Project GDR Users Handbook, Report D-8944, (Jet Propuls Labs, Pasadena, California) 1992, pp. 84.
- 10 Tapley B D, Ries J C, Davis G W, Eanes R J, Schutz B E, Shun C K, Watkins M M, Marshall J A, Nerem R S, Putney B H, Klosko S M, Luthcke S B, Pavlis, Williamson R G & Zelensky N P, *J Geophys Res*, 99 (1994) 24383.
- 11 Rapp R H, Wang Y M & Pavlis N K, *The OhioState 1991 geopotential and seasurface topography harmonic coefficient models*, Report 410, (Ohio State University, Columbus, Ohio) 1991, pp. 96.
- 12 Basic T & Rapp R H, *Oceanwide prediction of gravity anomalies and sea surface heights using Geos-3, Seasat and Geosat altimeter data and ETOPOSU bathymetric data*, Report 416, (Ohio State University, Columbus), 1992.
- 13 Prasanna Kumar S & Prasad T G, *Curr Sci*, 71 (1996) 834.
- 14 Legeckis R, *J Geophys Res*, 92 (1987) 12974.
- 15 Shetye S R, Gouveia A D, Shenoi S S C, Sundar D, Michael G S & Nampoothiri G, *J Geophys Res*, 98 (1993) 945.
- 16 Unnikrishnan K S, Prasanna Kumar S & Navelkar G S, *J Mar Res*, 55 (1997) 93.
- 17 Antony M K & Unnikrishnan K S, *Pacific Ocean Remote Sensing Conference (PORSEC I) Proceedings*, Okinawa, 1992, 527.
- 18 Prasanna Kumar S, Snaithe H M, Callenor P G & Guymer T H, Signatures of Kelvin and Rossby waves in the tropical Indian Ocean from TOPEX/POSEIDON altimeter, (under preparation).
- 19 Jones M S, *The circulation of the south Atlantic and its response to atmospheric forcing observed by spaceborne sensors*, Transfer Thesis, (James Rennell Centre for Ocean Circulation, Southampton) 1994, pp. 21.